The 2010 IEEE/RSJ International Conference on
Intelligent Robots and Systems
October 18-22, 2010, Taipei, Taiwan

# Master-Slave Robotic System for 3 dimensional Needle Steering

Hyo-Jeong Cha, Jaeheon Chung, Whee Kuk Kim, and Byung-Ju Yi

*Abstract*—**This paper proposes a new 4-Degree-of-Freedom (DOF) master-slave system for 3 dimensional needle steering. Both master and slave devices are commonly composed of a 3 DOF spherical type parallel mechanism and a 1 DOF needle insertion mechanism. This system provides users with 3 dimensional needle steering and force reflection capabilities. The real time forward solution of the master device is addressed. The design of the master-slave system is described in detail. Finally, the effectiveness of this system for 3 dimensional needle steering task is verified through experimental work.**

## I. Introduction

NEEDLE insertion is an important aspect of many medical diagnosis and treatments. Also, recently, the trend of contemporary medicine is toward less invasive surgery. Needle insertion task is one of typical tasks in many minimally invasive surgeries. It is very important to move a needle freely in a limited, affected area; nevertheless, some of needle steering mechanisms have one or two DOFs [1-3], so they are not adequate to perform the needle insertion task requiring more motion DOFs.

On the other hand, Fichtinger, *et al.* [4], Masamune, *et al.* [5], and Emad, *et al.* [6] proposed serial type needle placement devices that have more than six DOFs. They belong to typical serial type of needle insertion devices and are classified as floating needle insertion devices in that the robot is not mounted on the patient's body, but it is attached to the end of the medical robot. Note that the da Vinci surgical system employs a similar design concept. However, stiffness for this type of serial needle insertion devices is relatively low and also its accuracy is relatively low due to its cantilever structure. Thus, they may not be suitable for tasks requiring very high precision or for tasks under external disturbances.

As one of efforts to resolve the drawbacks mentioned above, Chung, *et al.* [7] proposed the 4 DOF parallel mechanism, which is composed of a 3 DOF spherical type parallel mechanism and a 1 DOF needle insertion mechanism. Merits of this device are that the motion DOFs and the needle insertion task can be achieved with one mechanism module and the platform is attachable to skin. Thus, compared to previous needle insertion devices, the mechanism is compact and resolves the problem of floating type needle insertion device.

A proper master device is required to implement such a needle insertion device to a real clinic. This paper proposes a proper master device to control this slave device and a master-slave control system. The parallel mechanism has been extended its applications to master devices since it has nice features such as its low inertia, which could be achieved by locating heavy actuators toward the ground, its high stiffness and etc. There have been many parallel mechanism designs proposed in literature for master devices [8-11]. Particularly, a spherical type parallel mechanism was attempted as the master device [12]. Another master device using the 4 DOF spherical parallel mechanism is proposed by Park, *et al.* [13], which has less singularity and better isotropy. Using the same kinematic structure, Yi, et al. [14] proposed to use a redundantly actuated spherical shoulder mechanism for fault tolerant operation, which enhances the force transmission capability.

In order to realize the 3 dimensional needle steering operation using the master-slave robotic system proposed in this paper, the forward kinematics of the master device should be derived firstly. Then, the output angles obtained by the forward kinematics are provided as a output position command to the slave device which follows the master device through conducting the inverse kinematics. On the other hand, the force generated by needle insertion is measured by a force sensor attached to the slave robot and it is fedback to the operator by the actuator mounted on the platform of the master robot.

The main goal of this bilateral control process is to make a user conduct an operation of steering and inserting the needle easily and intuitively as possible. Particularly, a different and promising feature of this work from the previous needle steering researches [1-6, 15-18] is that the current system could conduct the 3 dimensional needle steering operations naturally. In fact, steering a bevel-tip needle by a rotary actuator in the previous systems [15-18] tends to limit workspace inside biological tissues in actual operation. However, regardless of the types of needles (bevel or straight tip, stiff or flexible needle), the proposed master-slave needle insertion system could provide the user with a more natural and general needle steering capability.

The contents of this work are summarized as follows. In section II, the master device is introduced and its forward kinematic model is derived. The slave device is introduced in section III. Experimentation of the 4-DOF master-slave system is conducted in section IV. Finally, section V draws the conclusion.

H.-J. Cha is with School of Electrical Engineering and Computer Science, Hanyang University, Ansan, Korea. (e-mail: hyojeongcha84@gmail.com).

J.-H. Chung is with Department of Advanced Medical Initiatives, Faculty of Medical Sciences, Kyushu University, Japan. (e-mail: jaeheon.chung@gmail.com)

W.K. Kim is with Department of Control and Instrumentation Engineering, Korea University, Seoul, Korea. (e-mail: wheekuk@korea.ac.kr)

B.-J. Yi is with School of Electrical Engineering and Computer Science, Hanyang University, Ansan, Korea. (corresponding author phone: +82-31-400-5218; fax:+82-31-416-6416; e-mail: bj@hanyang.ac.kr)

## II. Design of a Master Device

### A. Description of the Master Device

Fig. 1 depicts a parallel mechanism that generates 3 DOF spherical motions by using redundant actuation (i.e., 4 actuators). It consists of a top platform and four serial sub-chains connected to it. Each of the four serial sub-chains consists of two links and three revolute joints. The direction of each joint axis can be denoted as the unit vector $S_n^m$, where the superscript $m$ and the subscript $n$, respectively, denotes the sub-chain and the joint location in the specified sub-chain. Note that this vector represents the unit vector along the z-axis of the corresponding local frame. Also, all $S_n^m$ vectors

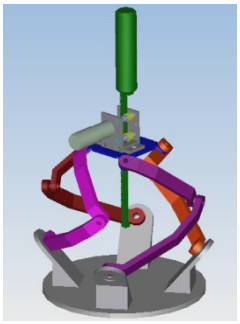

Fig. 1. The 3 DOF master device.

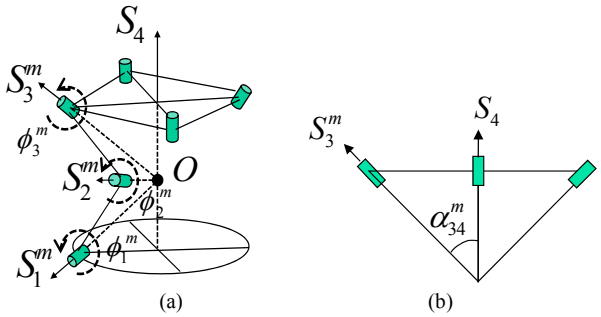


Fig. 2. Kinematic parameters of the master mechanism. (a) One serial chain (b) Side view of the top platform.

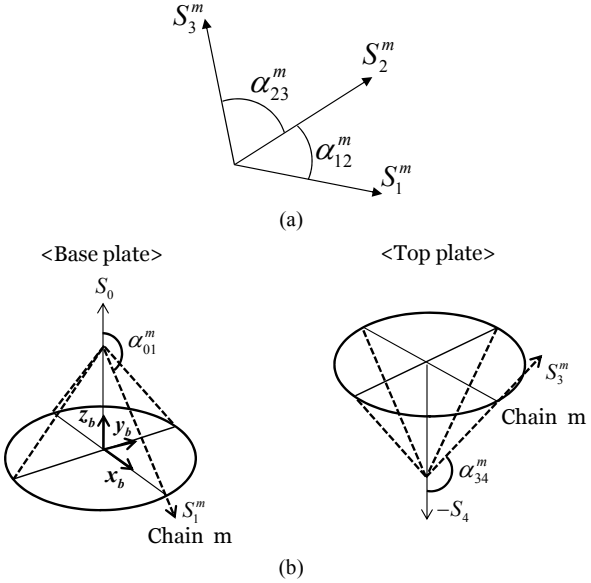


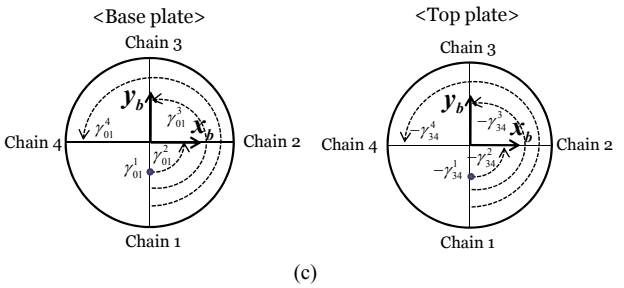


(c)

Fig. 3. Twist angle, Apex angle, and Edge displacement angle. (a) Twist angles (b) Apex angles (c) Edge displacement angles.

intersect at the common intersection point where the origins of all local frames including both the base frame and global frame are located at the center $O$ of the mechanism as shown in Fig. 2.

The vectors $a_{jk}^m$ (for $j,k=1,2,3$) representing the unit vector, respectively, along the x-axis of the corresponding local frames and are defined along the direction commonly perpendicular to those two neighboring $S$ vectors as follows:

$$a_{01}^m = S_1^m \times S_0,\ \ a_{12}^m = S_1^m \times S_2^m,\ \ a_{23}^m = S_2^m \times S_3,\ \ a_{34}^m = S_4 \times S_3.$$

The twist angle $\alpha_{jk}^m$, representing the angle between two neighboring $S$ vectors about the vector $a_{jk}^m$, is defined by

$$\alpha_{jk}^m = \cos^{-1}(S_j^m \cdot S_k^m).$$

Remark that the twist angle shown in Fig. 3(a) is one of important design parameters of the shoulder mechanism in aspect of size and shape of the workspace. The parameters describing the edge displacement angle of the base and the top links are denoted as $\gamma_{01}^m$ and $\gamma_{34}^m$ (see Fig. 3(c)), respectively.

### B. Forward Kinematics of the Master Device

Forward kinematics is to find the output position and orientation of the mechanism when the input variables are known. The output pose of the top plate of the master device is represented as x-y-z Euler angles ($\mu_1, \mu_2, \mu_3$) as shown in Fig. 4.

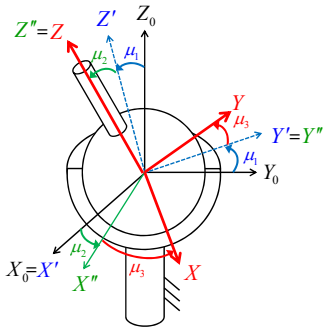


Fig. 4. Euler angle rotations.

The output rotation matrix $[R_o]$ is expressed as

$$[R_o] = [Rot(X,\mu_1)][Rot(Y,\mu_2)][Rot(Z,\mu_3)]. \qquad (1)$$

The output rotation matrix $[{}_mR_0^t]$ of each sub-chain which can be expressed as

$$[{}_m R_0^t] = [{}_m R_0^b][{}_m R_b^1][{}_m R_1^2][{}_m R_2^3][{}_m R_3^t] \text{ for } m = 1,2,3,4, \quad (2)$$

where $m$ is the number of sub-chains and the rotation matrix of each local frame with respect to its previous local frame, from the base frame to the top frame in order, can be expressed as follows:

$$[{}_m R_0^b] = [Rot(Z, \gamma_{01}^m)][Rot(X, \alpha_{01}^m)],$$
$$[{}_m R_b^1] = [Rot(Z, \psi_1^m)],$$
$$[{}_m R_1^2] = [Rot(X, \alpha_{12}^m)][Rot(Z, \psi_2^m)],$$
$$[{}_m R_2^3] = [Rot(X, \alpha_{23}^m)][Rot(Z, \psi_3^m)],$$

and

$$[{}_m R_3^t] = [Rot(X, -\alpha_{34}^m)][Rot(Z, -\gamma_{01}^m)],$$

where

$$\psi_1^m = \phi_1^m + \pi/2,$$
$$\psi_2^m = \phi_2^m + \pi/2,$$

and

$$\psi_3^m = \phi_3^m - \pi/2.$$

Since (1) and (2) represents the same output orientation of the mechanism, the following equation holds

$$[R_o] = [{}_m R_0^b][{}_m R_b^1][{}_m R_1^2][{}_m R_2^3][{}_m R_3^t]. \quad (3)$$

Now, (3) can be rearranged as below:

$$[{}_m R_0^b]^T [R_o][{}_m R_3^t]^T \begin{bmatrix} 0 \\ 0 \\ 1 \end{bmatrix} = [{}_m R_b^1][{}_m R_1^2][{}_m R_2^3] \begin{bmatrix} 0 \\ 0 \\ 1 \end{bmatrix}. \quad (4)$$

For convenience, the left hand side of (4) is denoted as

$$[{}_m R_b^0]^T [R_0][{}_m R_4^3]^T \begin{bmatrix} 0 \\ 0 \\ 1 \end{bmatrix} = \begin{bmatrix} r_{13} \\ r_{23} \\ r_{33} \end{bmatrix}. \quad (5)$$

Then, from (4) and (5) the following two equations are obtained as below:

$$c\psi_1^m r_{13} + s\psi_1^m r_{23} = s\psi_2^m s\alpha_{23}^m \quad (6)$$

$$r_{33} = -s\alpha_{12}^m c\psi_2^m s\alpha_{23}^m + c\alpha_{12}^m c\alpha_{23}^m \quad (7)$$

Lastly, from (6) and (7) the final form of a constraint equation for the *m-th* chain is obtained as

$$f_m = \left(r_{33} - c\alpha_{12}^m c\alpha_{23}^m\right)^2 + \left\{s\alpha_{12}^m \left(c\psi_1^m r_{13} + s\psi_1^m r_{23}\right)\right\}^2 - \left(s\alpha_{12}^m s\alpha_{23}^m\right)^2 = 0. \quad (8)$$

Note that out of four constraints expressed as in (8), only three constraint equations are enough to compute three output variables ( $\mu_1$ , $\mu_2$ , and $\mu_3$ ). Particularly, since the proposed parallel mechanism has multiple forward position solutions (i.e., 8th order [19]), a numeral method is adopted to calculate the desired robot pose which turns out to be fast enough for real time applications as explained below. The output variable is obtained numerically using the Newton-Raphson method.

In order to verify the real time application of this numerical method, the computation time to calculate the forward position solution is estimated. The data transmission time from the master device to the slave device is measured as 10 milliseconds, but it takes only 50 microseconds to calculate the one forward position solution as shown in Fig. 5. Thus, the numerical method to solve the forward position of the proposed spherical mechanism is regarded acceptable for real time control.

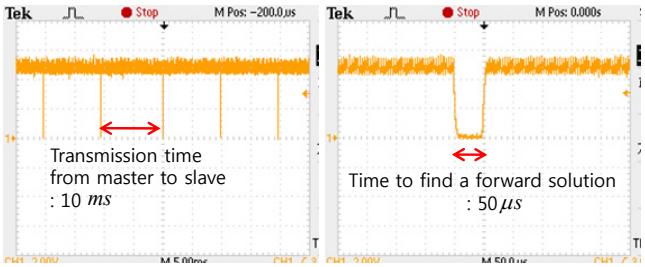


(a) (b)

Fig. 5. The computation time for one forward position solution. (a) Transmission time from the master to the slave (b) Time to find the forward position solution.

## III. Design of a Slave Device

### A. Description of the Slave Device

Fig. 6(a) shows the slave device adopted for our system. The slave device consists of a top plate, a base plate, four external legs with UPS structure (where U, P, and S, represents universal joint, prismatic joint, and spherical joint, respectively), and one internal leg with PS structure connecting those two plates. Particularly, this system was proposed as needle insertion device by Chung, et al. [7] and was investigated for singularity-free design along with its kinematic performance. Fig. 7 shows their prototype developed. According to their results, the offset angles, which represent the locations of the joint either on the base plate and on the top plate, need to be assigned as shown in Fig. 6(b) to secure large singularity-free dexterous workspace around its center. Thus, two offset angles need to be selected. $\mu_b$ and $\mu_t$ denote those two offset angles on the base plate and on the top plate, respectively.

Two promising merits of the slave device in Fig. 7 would be i) it provides the characteristic of RCM, the motion DOFs and the needle insertion task can be achieved only with one mechanism module, and ii) the platform is attachable to skin.

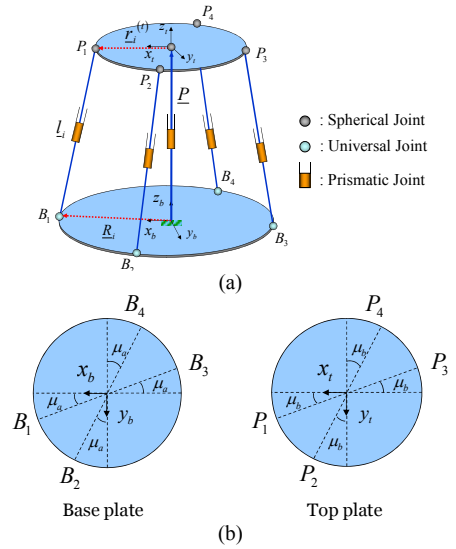


(a)

(b)

Fig. 6. The description of the slave mechanism.

Thus, compared to previous needle insertion devices, the mechanism is compact and resolves the problems of floating type needle insertion device.

### B. *Working Principle of the Slave Device*

With the mechanism shown in Fig. 6 being flipped upside down and the upper platform of this device could be attached to the skin. Fig. 7 shows the proposed configuration where a needle is being inserted to the skin through the hollow path guider in the middle chain, and exited through the ball joint located at the center of the lower plate. Note that through this path guider, the needle can be inserted manually by a user or inserted by an automatic insertion device with the human supervision particularly when a needle needs to be inserted through hard tissue region.

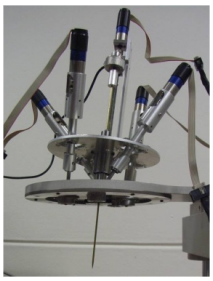

Fig. 7. The slave device.

The needle insertion process using the implemented mechanism can be explained as follows. First, the upper platform of this device is fixed to the target position of skin or body. Then, the mechanism is steered so that the needle can be oriented to the target direction. As a last step, the moving plate of the mechanism is pushed down so that the needle can be inserted into the skin. Note that the operating ranges of steering (or tilting) angle and roll angle of this device are confined within $\pm 25^{\circ}$ and $\pm 30^{\circ}$, respectively, mainly due to the mechanical limitations of spherical joints and mechanical interference.

## IV. Experimental System

### A. *The master-slave device*

Fig. 8(a) shows the master device. A handle is attached to the top of the needle part so the operator can grip and control the device more comfortably. Fig. 8(b) shows the needle insertion device. The device uses the rack and pinion transmission in which the handle and the needle are fixed to both ends of the rack and the motor drives a pinion gear. The maximum stroke of the handle is 130mm. Note that the master device not only derives the needle but also has reflecting force capability. In fact, there are various types of needles (bevel or straight tip, stiff or flexible needle) which could be employed in our master device. However, in this experiment, we employ a stiff and straight needle rather than using a flexible needle [15-18] with a bevel tip.

Fig. 9 shows the needle driving mechanism mounted on the platform of the slave device. A 1 DOF force sensor is attached to the end of the needle to measure the contact force generated by the needle insertion into a skin. Both the needle and the force sensor are moved by a lead screw. The maximum stroke of the needle is 80mm. Fig. 9 shows the detailed design of the needle insertion mechanism.

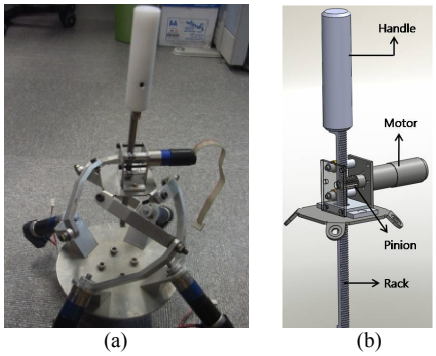


(a) (b)

Fig. 8. The proposed master device. (a) Master device (b) Needle insertion device.

### B. *Tele-operation Experiments*

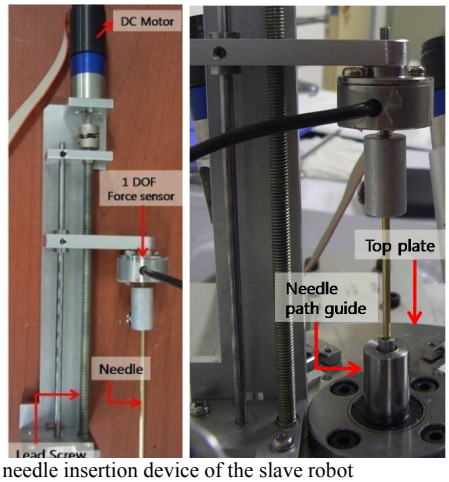


Fig. 9. The needle insertion device of the slave robot

Fig. 10 shows the master-slave robotic system implemented for the 3 dimensional needle steering operation. Fig. 11 and Fig. 12 show the block diagram of the control system and the controller for this system, respectively. Since the workspace of the master device is larger than one of the slave device, the motion scale factor of 2:1 is applied to the movement of the slave robot.

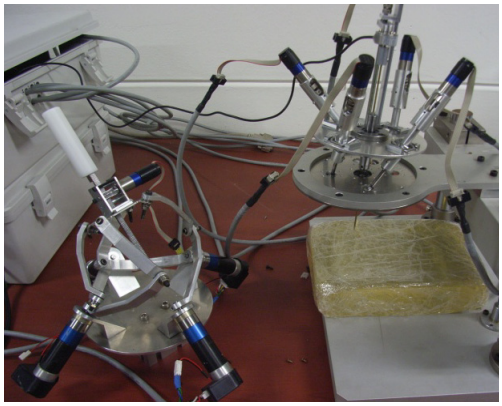

Fig. 10. The master-slave system for the needle insertion experiment.

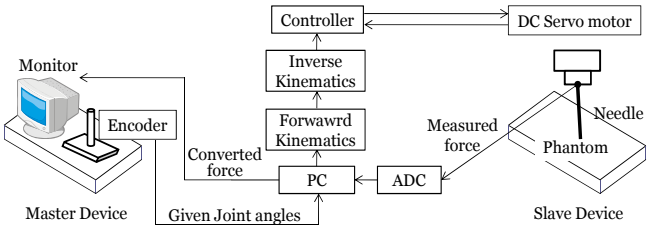


Fig. 11. The block diagram of the master-slave control system.

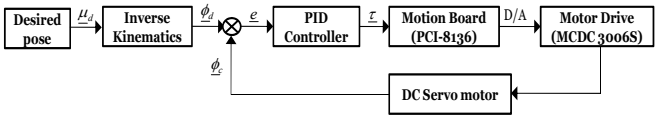


Fig. 12. The controller design.

### C. *Experimental Results*

Experiments on a master-slave position control are performed. As a first step, the operator moves the master robot to align the needle of the slave robot to the direction of the target point inside the phantom before penetrating the needle into the surface of the phantom. The attached video clip demonstrates the synchronized motion of the master-slave system. Once alignment is done, both the poses of the slave robot and the master device are fixed.

Then, the needle of the slave robot is being inserted into the phantom as shown in Fig. 13 through moving the needle of the master device. The phantom tissue is made of gelatin which is visco-elastic, and it is wrapped with layers of vinyl papers so that they mimic a human skin. The depth of the phantom tissue is 60mm. Note that in general, the stiffness of the skin is stiffer than that of biological tissues. Fig. 14 shows the measured force in this needle insertion experiment. This experiment result shows that the measured force before penetration of the needle into the skin is larger than the one after penetration. A similar phenomenon was reported in [20]. Thus, it can be confirmed that this phantom tissue can be employed as a virtual human tissue.

As mentioned in section III, the slave mechanism provides the characteristic of RCM. Thus, in the third experiment, we performed the 3 dimensional needle steering operation as RCM. Fig. 15 shows that using the 3 DOF spherical motion of the slave mechanism, the user is able to steer the needle inside the phantom. Fig. 16 shows the measure force in this experiment.

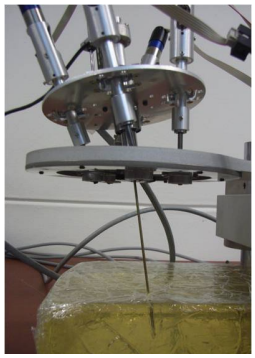

Fig. 13. Experiment for needle insertion.

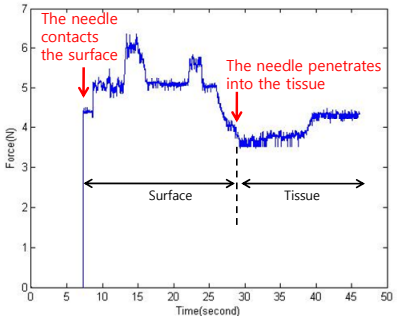


Fig. 14. The force generated by inserting the needle.

Lastly, a complete experiment consisting of insertion of the needle and tracking a target via master-slave control is performed. A piece of almond embeded into the gelatin is considered as a target. The phantom is set under the base plate of the slave device. The experiment procedure is as follows.

(1) Control the orientation of the master robot so that the needle of the slave robot is aligned to the direction of the target inside the phantom.
(2) Insert the needle into the phantom by controlling the needle insertion drive and check the position error visually.
(3) Make an adjustment of steering the needle inside the phantom so that the needle is aligned to the target.
(4) Repeat (2) and (3) until the needle hits the target.

Fig. 17 shows some of snap pictures during this operation, and the attached video clip demonstrates the whole procedure of this experiment.

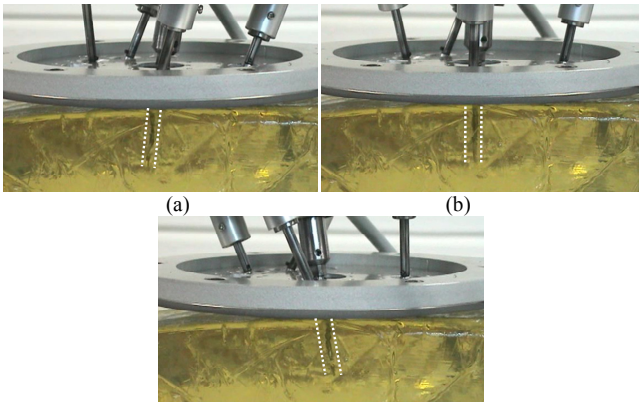


Fig. 15. Experiment for the RCM motion. (a) The needle was steered to the left (b) The needle was inserted straightly (c) The needle was steered to the right.

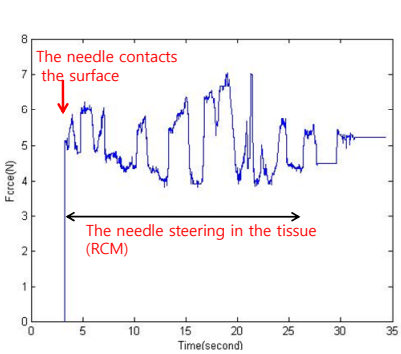


Fig. 16. The force measured during the target tracking experiment.

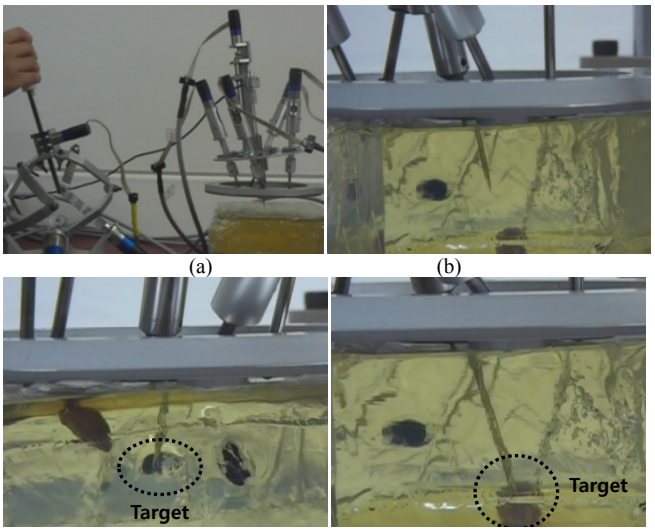


Fig. 17. The target tracking experiment. (a) The position control (b) The needle insertion (c) The 3 dimensional needle steering.

## V. CONCLUSION

A new 4-DOF master-slave system having three rotational motions and one needle insertion motion was proposed. Proto type of the master-slave system for the 3 dimensional needle steering task was developed and tested to confirm effectiveness of the proposed system. A promising feature of this work over previous needle steering researches [1-6, 15-18] is that the proposed system has capability of the 3 dimensional needle steering. Steering a bevel-tip needle by a rotary actuator provides a limited workspace inside biological tissues. Nonetheless the type of needles (bevel-tip or straight tip), the proposed master-slave needle insertion system provides the user with a general needle steering capability. Future work involves a diagnosis of the biological organ by the force measurement and the feedback control of the needle insertion force during a special clinical operation of biological organs.

## ACKNOWLEDGEMENT

This work was partially supported by Mid-career Researcher Program through NRF grant funded by the MEST (No. 2010-0000247), partially supported by GRRC program of Gyeonggi Province (GRRC HANYANG 2010-A02), partially supported by the Ministry of Knowledge Economy (MKE) and Korea Industrial Technology Foundation (KOTEF) through the Human Resource Training Project for Strategic Technology, and the outcome of a Manpower Development Program for Energy & Resources supported by the Ministry of Knowledge and Economy (MKE).

## REFERENCES

[1] K. Podder, et al. "Evaluation of robotic needle insertion in conjunction with in vivo manual insertion in the operating room," in *Proc. IEEE Int. Workshop Robots Human Interactive Commu.*, 2005, pp. 66-72.

[2] S. P. DiMaio and S. E. Salcudean, "Simulated interface needle insertion," in *Proc.10th Symp. Haptic Interfaces for Virtual Envir. & Teleoperator System.*, 2002.

[3] C. M. Schneider, A. M. Okamura, and G. Fichtinger, "A robotic system for transrectal needle insertion into the prostate with integrated ultrasound," in *Proc. Int. Conf. Robot. Autom.*, 2004, pp. 365-370.

[4] G. Fichtinger, J. Fiene, C. Kennedy, I. Iordachita, G. Kronreif, D. Y. Song, E. C. Burdette, and P. Kazanzides, "Robotic assistance for ultrasound guided prostate brachytherapy," *Med. Image Anal.*vol. 12, no. 5, 2009, pp. 535-545.

[5] K. Masamune, G. Fitchtinger, A. Patriciu, R. C. Susil, R. H. Taylor, L. R. Kavoussi, J. H. Anderson, I. Sakuma, T. Dohi, and D. Stoianovici, "System for robotically assisted percutaneous procedures with computed tomography guidance," *J. Comput. Aided Surg*., vol. 6, no. 6, 2001, pp. 370-383

[6] E. M. Boctor, R. J. Webster III, H. Mathieu, A. M. Okamura, and G. Fichtinger, "Virtual remote center of motion control for needle-placement robots," *Computer-Aided Surgery*, vol. 9, no. 5, 2004, pp.175-183.

[7] J. Chung, H.-J. Cha, B.-J. Yi and W. K. Kim, "Implementation of a 4-DOF parallel mechanism as a needle insertion device," in *IEEE Int. Conf. Robot. Autom.*, 2010, pp.662-668.

[8] J. Yoon and J. Ryu, "Design, fabrication, and evaluation of a new haptic device using a parallel mechanism," *IEEE/ASME Trans. on Mechatronics*, vol. 6, no. 3, September, 2001, pp.221-233.

[9] S.-U. Lee and S. Kim, "Analysis and optimal design of a new 6 DOF parallel type haptic device," in *Proc. Int. Conf. Intell. Robot. Syst*., 2006, pp.460-465.

[10] J.-W. Kim, D.-H. Park, H.-S. Kim, and S.-H. Han, "Design of a novel 3-DOF parallel type haptic device with redundant actuation," *Int. Conf. Control, Autom. Syst*., 2007, pp. 2270-2273.

[11] J. Arata, H. Kondo, M. Sakaguchi, and H. Fujimoto, "Development of a haptic device "DELTA-4" using parallel link mechanism," *Int. Conf. Robot. Autom*., 2009, pp.294-300.

[12] L. Birglen, C. Gosselin, N. Pouliot, B. Monsarrat, and T. Laliberte, "SHaDe, a new 3-DOF haptic device," *IEEE Trans. Robot. Autom*., vol. 18, no. 2, April, 2002, pp.166-175.

[13] B.-J. Park, B.-J. Yi and W. K. Kim, "Design and analysis of a new parallel grasper having spherical motion," in *Proc. Int. Intell. Robots Syst*., 2004, pp. 106-111.

[14] B.-J. Yi, D. Tesar, and R.A. Freeman, "Analysis of a redundantly actuated fault-tolerant spherical shoulder module," in *Proc. ASME* 22st Biennial Mechanism Conf., 1991.

[15] O. Piccin, L. Barbe, B. Bayle, M. de Mathelin, and A. Gangi, "A force feedback teleoperated needle insertion device for percutaneous Procedures," *The International Journal of Robotics Research,* vol. 28, no. 9, pp.1154-1168, September, 2009.

[16] J. Rober, R. J. Webster III, J. S. Kim, N. J. Cowan, G. S. Chirikjian, and A. M. Okamura, "Nonholonomic modeling of needle steering," *The International Journal of Robotics Research*, vol. 25, no. 5-6, pp. 509-525, May-June, 2006.

[17] J. M. Romano, R. J. Webster III, and A. M. Okamura, "Teleoperation of steerable needles," in *Proc. IEEE Int. Conf. on Robotics and Automation*, 2007, pp. 934-939.

[18] D. Glozman and M. Shoham,"Flexible needle steering for percutaneous therapies," *Computer-Aided Surgery*, vol. 11, no. 4, pp. 194-201, 2006.

[19] Merlet,J.-P., *Parallel Robots*, Kluwer Academic Publishers, 2000.

[20] A. M. Okamura, C. Simone, and M. D. O'Leary, "Force modeling for needle insertion into soft tissue," *IEEE Transactions on Biomedical Engineering*, vol. 51, no. 10, pp.1707-1716, Oct, 2004.